A numerical alignment error estimation for the SPring-8-II

Y. Okayasu*, H. Kimura
Japan Synchrotron Radiation Research Institute, Sayo-gun, Hyogo, 679-5198, Japan
S. Matsui
RIKEN SPring-8 Center, Sayo-gun, Hyogo, 679-5198, Japan

Abstract

Alignment errors for entire accelerator components of the SPring-8-II configuration are numerically estimated and confirmed to satisfy required allowable errors. Necessity of realignment are also discussed tracking both estimated observation coordinates and relative errors of neighboring two common girders based on ground deformation trends of SPring-8. Furthermore, a verification of the ATL-law application for variations of the current storage ring level is briefly introduced and discussed.

INTRODUCTION

One of targets of the SPring-8 storage ring upgrade plan (SPring-8-II) is to realize an ultra-low emittance ring which requires severe allowable alignment errors (peak-to-peak) in horizontal plane, such as ± 30 μm (desired value) for multi-pole magnets on common girders and ± 90 μm for neighboring two common girders.

Goals of this study are to answer following three questions; 1) whether our conventional methods of alignment and survey will satisfy allowable alignment errors, 2) do we need additional observation points and vise versa? 3) Frequency of the realignment.

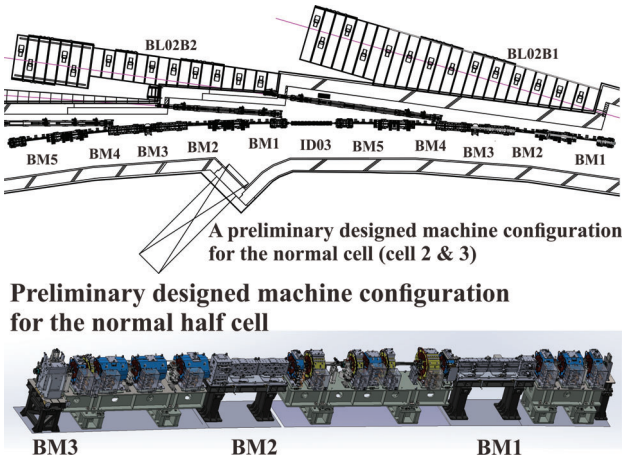

Figure 1: Top view of a preliminary designed machine configuration for the normal cell (*upper*) and its 3D model for the normal half cell (*lower*). Any correction magnets excepted in these above figures.

In order to answer these above questions, a ground deformation of SPring-8 storage ring has been estimated based on survey data for accelerator components which has been continuously measured since 1996 [1]. Next, coordinates of all accelerator components, which is assumed as the SPring-8-II configuration as shown in Fig. 1, are numerically evaluated with the ground deformation estimation and instruments' errors assuming our current survey method. Necessity of the realignment are also discussed.

ALIGNMENT ERROR ESTIMATIONS FOR ACCELERATOR COMPONENTS

Observations of accelerator components' coordinates A_{obs} are briefly expressed as

$$A_{\mathrm{obs}} = A_{\mathrm{des}} + \Delta A_{\mathrm{top}} + \Delta A_{\mathrm{env}} \pm \sigma_{\mathrm{meas}} \qquad (1)$$

where A_{des} is designed coordinates. ΔA_{top} is correction term for topographical effects such as ground deformations. ΔA_{env} is also correction term for environmental effects such as temperature and pressure in the tunnel which is treated as zero in this study. σ_{meas} is measurement errors. In case of discussing alignment errors while their installation within short period, ΔA_{top} is negligible. Therefore, we need to discuss only σ_{meas} in principal and focus on it in this section. Comprehensive discussion including topographical effects is discussed in the next section.

Alignment errors for neighboring two girders are defined as sizes of relative error ellipses which are calculated by a network analysis with designed coordinates of two quadrupole magnets mounted at both ends of common girders. The calculation is processed using a code, which was developed based on Microsoft Visual Basic and distributed for free by S. Matsui [2], assuming following three conditions;

1) $\sim$1.5 km long tunnel ring consists of 44 normal cells and 4 straight sections, total 48 cells. 526 observation points are defined on quadrupole magnets at both ends of each common girder, 51 points on support columns on each insertion devices (IDs) and 204 points on both internal and external circumference wall in the ring. Observation points on the wall are designed to be distanced at regular intervals in the ring. Four standard IDs are assumed to be installed at each long straight section.

2) Survey method is following our current method, i.e., Leica AT-402 laser tracker is used for horizontal co-

* okayasu@spring8.or.jp

ordinates of all 781 observation points with 96 instrument points and Trimble DiNi0.3 digital level for levels of 48 observation points located on the center of normal cells and straight sections with 48 instrument points.

3) Errors (σ) for both angle and distance measurements in the calculation are treated as 0.57 arcsec and $\pm$7.6 μm + 2.5 μm/m, respectively based on current analysis results.

Also, in this paper, a definition of the coordinate system is Cartesian coordinate system with $+x$ for toward the east, $+y$ for the north and $+$z for the upward vertical direction. The origin are defined at the center of the storage ring.

The code processes two dimensional survey network analysis with both angle and distance measurement errors and coordinates of both observation and instrument points by linking them individually. Specifically, algebra utilized in the code starts from observation equations:

$$\boldsymbol{V} = \boldsymbol{A}\boldsymbol{X} - \boldsymbol{L} \tag{2}$$

where $\boldsymbol{L}$ and $\boldsymbol{X}$ are vectors of observed coordinates and optimal solutions, respectively. $\boldsymbol{V}$ is the vector of residuals and $\boldsymbol{A}$ is the coefficient matrix. In case of surveying by more than two instruments with different surveying accuracies, Eq. (2) can be described as

$$\boldsymbol{P}\boldsymbol{V} = \boldsymbol{P}\boldsymbol{A}\boldsymbol{X} - \boldsymbol{P}\boldsymbol{L} \tag{3}$$

taking into account weight factors $\boldsymbol{P}$ for instruments. Not only our code, general network analysis solves the observation equation minimizing the weighted residuals; $\partial \boldsymbol{V}^T \boldsymbol{P}\boldsymbol{V}/\partial \boldsymbol{X} = 0$. Finally, optimal solutions can be evaluated by solving the normal equation:

$$\begin{aligned} \frac{\partial \boldsymbol{V}^{\mathrm{T}}\boldsymbol{P}\boldsymbol{V}}{\partial X} &= 2\boldsymbol{A}^{\mathrm{T}}\boldsymbol{P}\boldsymbol{A}\boldsymbol{X} + \boldsymbol{A}^{\mathrm{T}}\boldsymbol{P}\boldsymbol{L} + (\boldsymbol{L}^{\mathrm{T}}\boldsymbol{P}\boldsymbol{A})^{\mathrm{T}} = 0 \\ &\rightleftharpoons \quad \boldsymbol{A}^{\mathrm{T}}\boldsymbol{P}\boldsymbol{A}\boldsymbol{X} - \boldsymbol{A}^{\mathrm{T}}\boldsymbol{P}\boldsymbol{L} = 0 \\ &\rightleftharpoons \quad \boldsymbol{X} = (\boldsymbol{A}^{\mathrm{T}}\boldsymbol{P}\boldsymbol{A})^{-1}\boldsymbol{A}^{\mathrm{T}}\boldsymbol{P}\boldsymbol{L}. \end{aligned} \tag{4}$$

Here, $\boldsymbol{V}^{\mathrm{T}}\boldsymbol{P}\boldsymbol{V}$ is a symmetric and variance-covariance matrix which consists of variance components C_{ii} and covariance components $C_{ij}(i \neq j)$. Both i and j are observation point identification numbers. Matrix element C_{ij} can be given with the standard deviation σ_{X_i} (X_i: x_i and y_i) for individual optimal solution as [3]:

$$C_{ij} \propto \sigma_{XiXj}. \tag{5}$$

Further details of algebra for the network analysis are described in [3, 4].

All continuous optimal solutions of observation points on the entire circumference can be derived from discrete measured data sets via processes described above. Residual errors of each individual observed coordinate (absolute errors) and relations between neighboring two observations (relative errors) can be estimated independently by matrix elements C_{ij}. The former can be described by variance matrix elements C_{ii} only and the latter by covariance matrix elements C_{ij} ($i \neq j$).

These absolute or relative errors of observation coordinates can be discussed more efficiently with graphical representations by computing two dimensional error ellipses in one plane (usually in horizontal plane). Regardless of absolute or relative cases, important error ellipse parameters can be expressed as

$$s = \sqrt{\frac{t_1}{2} + \sqrt{\frac{t_2^2}{4} + t_3^2}} \tag{6}$$

$$l = \sqrt{\frac{t_1}{2} - \sqrt{\frac{t_2^2}{4} + t_3^2}} \tag{7}$$

$$\theta = \frac{1}{2}\tan^{-1}\left(-\frac{2t_3}{t_2}\right). \tag{8}$$

Here, s, l and θ are half-minor and half-major axes of error ellipse in sigma and the angle between half-major and x axes. Contents of t_1, t_2 and t_3 are defined separately in case of absolute and relative error ellipses as below.
Absolute error ellipse:

$$\begin{cases} t_1 = \sigma_{xi}^2 + \sigma_{yi}^2 \\ t_2 = \sigma_{xi}^2 - \sigma_{yi}^2 \\ t_3 = \sigma_{xiyi} \end{cases} \tag{9}$$

Relative error ellipse:

$$\begin{aligned} \sigma_{\Delta x}^2 &= \sigma_{xi}^2 - 2\sigma_{xixj} + \sigma_{xj}^2 \\ \sigma_{\Delta y}^2 &= \sigma_{yi}^2 - 2\sigma_{yiyj} + \sigma_{yj}^2 \\ \sigma_{\Delta x \Delta y} &= \sigma_{xiyi} - \sigma_{xiyj} - \sigma_{xjyi} + \sigma_{xjyj} \end{aligned}$$

$$\begin{cases} t_1 = \sigma_{\Delta x}^2 + \sigma_{\Delta y}^2 \\ t_2 = \sigma_{\Delta x}^2 - \sigma_{\Delta y}^2 \\ t_3 = \sigma_{\Delta x \Delta y} \end{cases} \tag{10}$$

Therefore, alignment errors for neighboring two common girders can be estimated by relative error ellipses of two quadrupole magnets coordinates.

Figure 2 shows half-major (*solid-blue*) and half-minor (*dashed-red*) axes of relative error ellipses on the entire circumference of the storage ring excepting all IDs. Both half-major and half-minor axes are relatively larger at four straight sections: cell 6, 18, 30 and 42 which are considered that due to the sparse network. Averages of half-major and half-minor axes are 18 μm and 17 μm, respectively, thus averaged alignment errors for neighboring two common girders are estimated to be $\sqrt{18^2 + 17^2} \simeq 25$ μm and at most 28 μm for straight sections. For vertical direction, the measurement error is estimated as 26 μm (σ) based on our survey results for elevation difference. Since the required allowable errors are $\pm$90 μm in peak-to-peak, i.e., $90/2\sqrt{2} \simeq 32$ μm in rms, estimated alignment errors for both horizontal and vertical directions are confirmed to be within the allowable errors. For visual understanding,

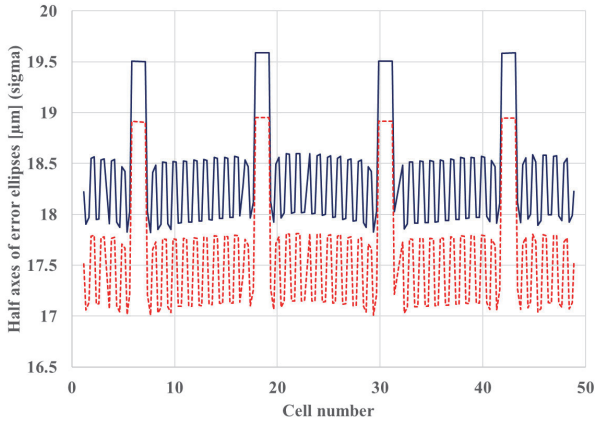

Figure 2: Calculated half-major (*solid-blue*) and half-minor (*dashed-red*) axes of relative error ellipses for the first accelerator components alignment.

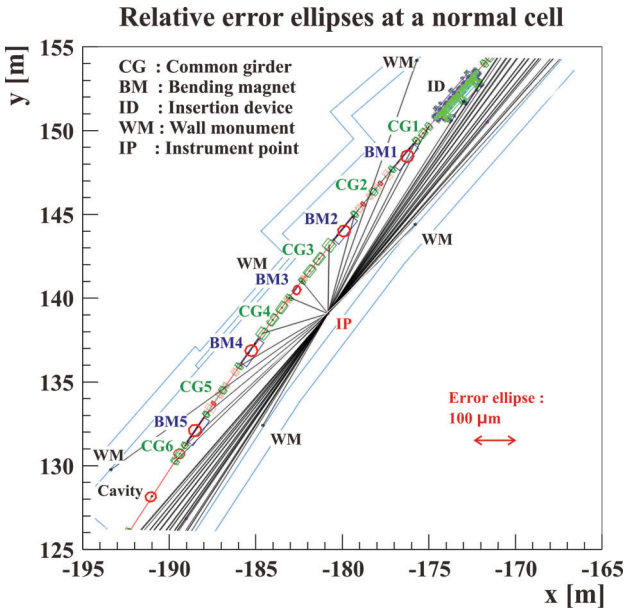

Figure 3: Calculated relative error ellipses overlaid on accelerator configuration at a normal cell.

Fig. 3 shows calculated relative error ellipses overlaid on designed accelerator configuration at one normal cell (Cell 13) with laser tracker trajectories. Further optimization especially for numbers and orientations of observation points on the tunnel wall are under review in order to improve alignment errors.

NECESSITY OF REALIGNMENT

A necessity of realignment for the SPring-8-II configuration is discussed in this section. In case that accelerator components are built in extremely stable environment, for example in deep underground, the realignment may not be required. However, since observation points of SPring-8 accelerator components are affected by ground deformations, i.e., the second term in the right form in Eq. (1), consideration of the realignment cannot be avoided.

Figure 4 shows trends of SPring-8 observation point level, which have been measured since 1996 to 2018, overlaid on ground contour-line map and infrastructures. Notations provided in Fig. 4 describe underground structures and ground constructions at locations of interest. Total 271 of observation point level trends are plotted along radial direction of the ring; inner of the ring starts from 1996 and outer ends by 2018. It is found that measured level is apparently reflected by underground structures and topography before the construction. It is interpreted that the ground level has been lifted up at most 2.5 mm at Cell 14 to 24 (ground cutting area) or sunk at most 1.5 mm at Cell 31 to 36 (banking area) over 20 years. Also, at most 1 mm sinking are recognized at underground constructions straddling the ring such as rainwater drain pipes, RF waveguides and underpasses.

Secular changes of relative error ellipses of the designed SPring-8-II accelerator configuration are calculated by tracking their components' coordinate variations in order to discuss the necessity of realignment. Designed coordinate variations are evaluated by linear interpolations and approximations via survey data sets, i.e. ground deformations, of SPring-8 over past 20 years assuming that the ground deformation is systematic and seasonal deformations is completely canceled.

First, deformation growth rates $a(s_j)$ of SPring-8 observation points $A_i(s_j)$, which have been surveyed since January 1996 to February 2018, are evaluated by linear approximations as

$$\Delta A_i^2(s_j) = \sum_i \left\{ A_i(s_j) - A'_i(s_j) \right\}^2 \quad (11)$$

$$A'_i(s_j) = a(s_j) i + b(s_j) \quad (12)$$

where A represents x, y and z of SPring-8 observation coordinates, i is passed year since January 1996 ($i = 1 \sim 22$) and j is observation point number ($j = 1 \sim 271$). s_j is the coordinate of j-th point on the designed beam orbit which origin is defined at the most upstream quadrupole magnet in the Cell 1. A linear approximated coordinate A' consists of the deformation growth rate a and the offset b of j-th point. The deformation growth rate and the offset are optimized to minimize Eq. (11).

Next, the deformation growth rate $a(s_k)$ of k-th ($k = 1 \sim 781$) SPring-8-II observation coordinates can be calculated by the linear interpolation with $a(s_j)$ as

$$a(s_k) = \frac{a(s_j) - a(s_{j-1})}{s_j - s_{j-1}} (s_k - s_{j-1}) + a(s_{j-1}) \quad (13)$$

and evaluated deformation growth rates for each SPring-8-II observation point are shown in Fig. 5.

Assuming that all observation coordinates of the SPring-8-II configuration in installation year as designed coordinates $A_0(s_k)$, their coordinates $A_l(s_k)$ after l-year later from the installation can be calculated by Eq. (12) with

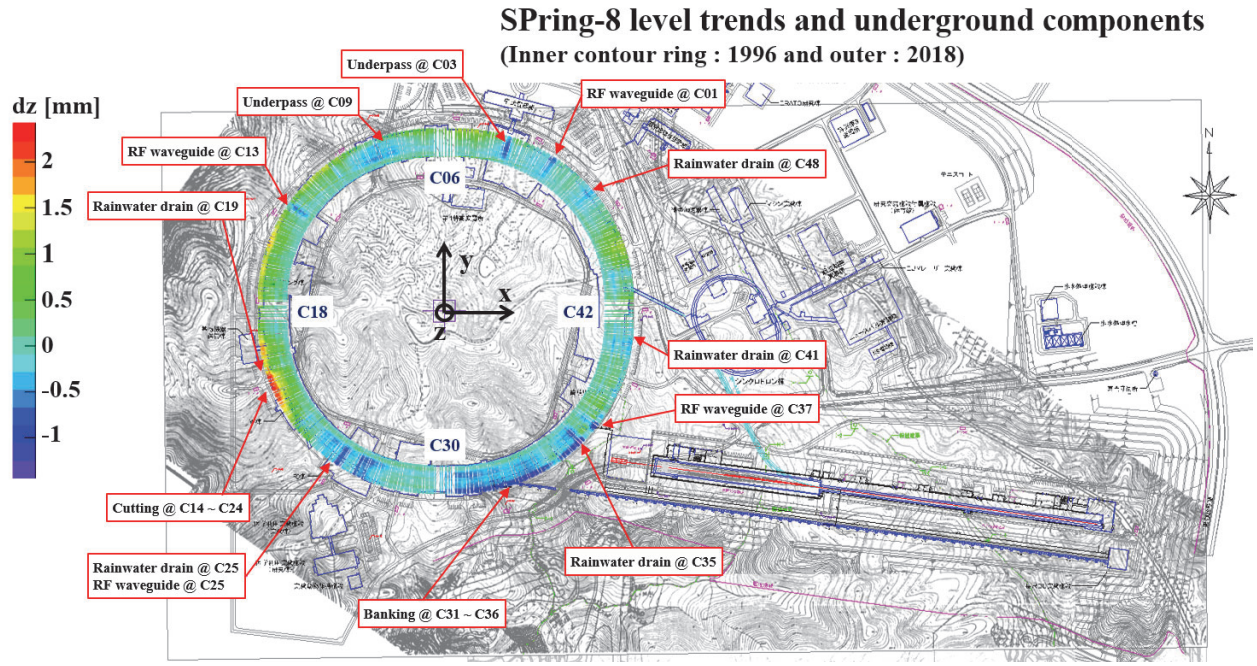

Figure 4: Measured SPring-8 accelerator component levels since 1996 overlaid on ground contour-line map and infrastructures. Radial direction of the contour ring represents passed year, i.e., inner of the ring starts from 1996 and outer ends by 2018. Shortened cell numbers are also provided as C06 for Cell 06. Typical length of the normal one cell is ∼30 m.

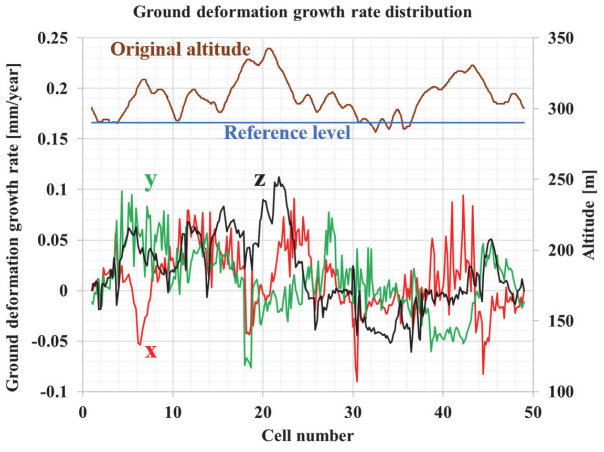

Figure 5: Evaluated ground deformation growth rates for x, y and z. Both the original altitude and the reference level along the beam orbit are also overlaid as reference.

ground deformation growth rates Eq. (13). Three dimensional residuals of coordinates $\Delta R(l)$ between observations and designed ones for neighboring two common girders after l-year later from the installation can be described as

$$\begin{aligned}\Delta R(l) &= \Big[\{dx_l(s_k) - dx_l(s_{k-1})\}^2 \\ &+ \{dy_l(s_k) - dy_l(s_{k-1})\}^2 \\ &+ \{dz_l(s_k) - dz_l(s_{k-1})\}^2\Big]^{\frac{1}{2}} \qquad (14)\end{aligned}$$

, where $dA_l(s_k) = A_l(s_k) - A_0(s_k)$, $(A = x, y, z)$. Now, $\Delta R(l)$ is separated into horizontal and vertical components as

$$\begin{aligned}\Delta R_{\rm hol}(l) &= \Big[\{dx_l(s_k) - dx_l(s_{k-1})\}^2 \\ &+ \{dy_l(s_k) - dy_l(s_{k-1})\}^2\Big]^{\frac{1}{2}} \qquad (15)\end{aligned}$$

$$\Delta R_{\rm ver}(l) = |dz_l(s_k) - dz_l(s_{k-1})|. \qquad (16)$$

Both $\Delta R_{\rm hol}(l)$ and $\Delta R_{\rm ver}(l)$ are calculated for total 263 of neighboring girders combinations and survival rates of combinations below the allowable alignment error; 90 μm are evaluated for 5 years after the installation as shown in Fig. 6. As shown in Fig. 6, the realignment is expected to be required within two years for both horizontal and vertical directions. Incidentally, the horizontal component can be discussed dividing to two components, i.e., azimuthal (beam direction) and radial components of the designed ring coordinate which are also overlaid in Fig. 6.
Much more strict alignment tolerance is required especially for radial coordinates comparing to azimuthal ones which are known to be susceptible to temperature changes.

INTERPRETATION OF THE GROUND ELEVATION WITH ATL-LAW APPROACH

Finally, we discuss ground elevation changes with the aspect of the ATL-law. As discussed above, we have almost 20 years of rich survey data sets for SPring-8 accelerator

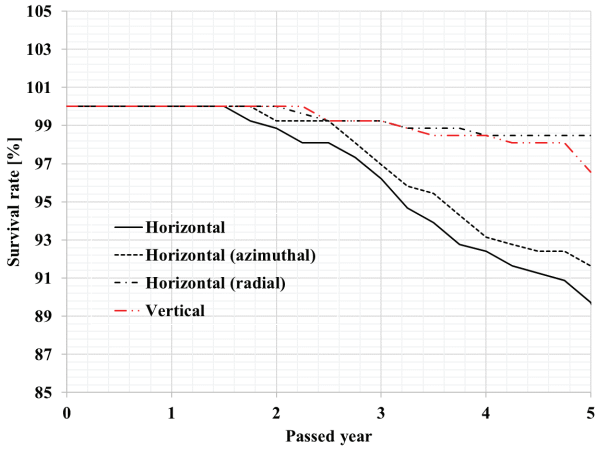

Figure 6: Survival rates of girder combinations (total 263) beneath allowable alignment errors; 90 μm for horizontal (*solid-black*) and vertical (*two-dot chain-red*) directions over 5 years. Both radial (*a-dot chain-black*) and azimuthal (*dashed-black*) components of horizontal direction are also overlaid.

components and found that there exists -1.5 $\sim$ 2.5 mm of ground elevation changes for this two decades.

Stochastic diffusive motion has been investigated in geophysics field which is considered to be one candidate to provide the ground motion among various well known natural factors; earth tides, activities of the geologic fault, periodic changes of temperature and pressure. Amplitude of the stochastic component is also considered to be much smaller comparing to other components and the motion is often treated as "random-walk" or Brownian motion. Thus, the component is discussed for relatively stable environment such as deep underground in general.

In accelerator physics, B. A. Baklakov *et al.* firstly proposed ATL-law to describe the variance of the ground elevation difference $\langle dz^2 \rangle$ between two points separated by distance L over a time interval T as [5]

$$\langle dz^2 \rangle \approx AT^{\alpha}L^{\beta}. \tag{17}$$

A is a coefficient which depends on the characteristic of the earth's crust. Both $\alpha \approx 1$ and $\beta \approx 1$ in Eq. (17) has been examined. Furthermore, V. D. Shiltsev intensively investigated the coefficient A for various accelerator facilities and so on except for SPring-8 [6].

Although, SPring-8 is constructed on the ground, it is widely recognized that the facility is built on relatively harder base rock comparing to other storage ring facilities. Therefore, we apply the ATL-law to the variance of elevation changes assuming that effects of day and night or seasonal temperature changes are averaged and canceled. Elevation change $dz(s)$ in the time interval T ($T = 1, \cdots, 22$) at a designed beam orbit coordinate s is described as

$$dz(T, s) = z(t + T, s) - z(t, s) \tag{18}$$

, where t is year of survey demonstrated. Now, variance of elevation changes for lag, i.e., distance between two points L with time interval T can be expressed as

$$\langle dz^2(T, L) \rangle = \frac{1}{M} \sum_{M} \frac{1}{N} \sum_{N} \{dz(T, s + L) - dz(T, s)\}^2. \tag{19}$$

N is pairs of points of circumference distanced by L and M is pairs of the time interval T. Figure 7 shows variances of elevation changes depend on the lag only up to 300 m comparing 1 year and 22 years change. One can find that the gradient is not unique especially for 22 year change.

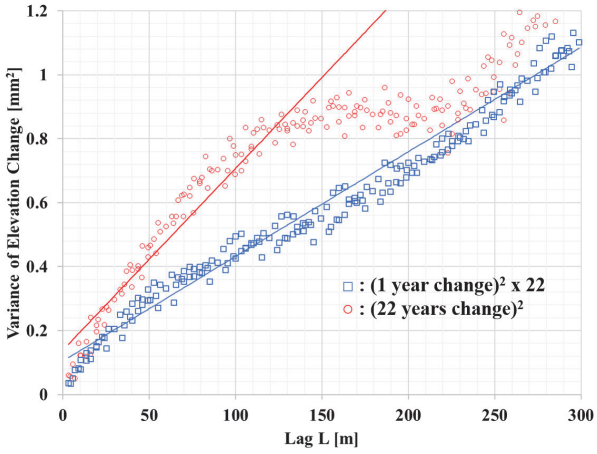

Figure 7: (Preliminary) Variances of SPring-8 ground elevation changes over time intervals of 1 year (multiplied by 22, *blue-rectangle*) and 22 years (*red-circle*) correlating with the lag L.

A reason of the gradient change is considered to be systematic, i.e., not random changes. One candidate can be expected as the continuous lift up at the ground cutting area or damping area which are distributed from Cell 14 to 24 ($\sim$300 m long) or Cell 31 to 36 ($\sim$150 m long), respectively as already shown in Fig. 4 and 5. Such that systematic changes should be excluded from data and further investigations are under go.

Gradients of variance of elevation changes for each time intervals are evaluated with errors from plots of Eq. (19) depending on the lag and plotted in Fig. 8.

Coefficient in the empirical ATL-law to characterize the earth's crust for SPring-8 storage ring is eventually estimated as $A_{\text{SPring-8}} = (9.0 \pm 1.5) \times 10^{-6}$ μm^2/s/m (preliminary).

SUMMARY

Alignment errors for neighboring two common girders designed as the SPring-8-II configuration is calculated and confirmed to satisfy required allowable errors via a two-dimensional network analysis. Numbers and orientation of observation points on the tunnel wall is still under optimizing to improve errors.

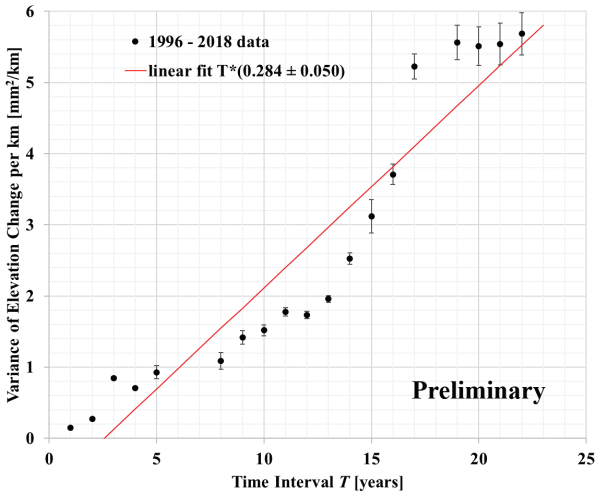

Figure 8: (Preliminary) Correlations between variances of SPring-8 ground elevation changes per unit distance and the time interval of the surveying.

Necessity of the realignment of SPring-8-II accelerator components are discussed based on the existing SPring-8 survey data measured over $\sim$20 years. As a result, it is estimated that the realignment will be required within at most 2 years.

Variance of elevation changes for the SPring-8 storage ring are discussed applying the empirical ATL-law which has never been estimated with $\sim$20 years of long period. The coefficient to characterize the earth's crust is also estimated. Further investigation for systematic effects, such as continuous lift up or damping associated with the ground construction, is in progress.

REFERENCES

[1] H. Kimura *et al.*, "Analysis of the vertical floor deformation in SPring-8 ring tunnel", Proc. International Workshop on Accelerator Alignment (IWAA), Grenoble, October 3-7 (2016).

[2] S. Matsui *et al.*, "Adjustment Program of the Horizontal Survey Network with Relative Error Ellipse", Proc. 12th Annual Meeting of PASJ, Tsuruga, Aug. 5-7 (2015), pp. 140-145.

[3] R. C. Smith and P. Cheeseman, "On the representation and estimation of spatial uncertainty", International Journal of Robotics Research, Vol. 5, No. 4 (1986), pp. 56-68.

[4] T. J. M. Kennie and G. Petrie, *Engineering Surveying Technology* (CRC Press, London, 1993).

[5] B. A. Baklakov *et al.*, Tech. Phys. **38**, 894 (1993).

[6] V. D. Shiltsev, Phys. Rev. Lett. **104**, 238501 (2010).